Moving Target Tracking with a Mobile Robot based on Modified Social Force Model

Qinxuan Sun
College of Artificial Intelligence,
Nankai University
Tianjin, China

Shengming Zhang
College of Artificial Intelligence,
Nankai University
Tianjin, China

Jing Yuan*
College of Artificial Intelligence,
Nankai University
Tianjin, China

Xuebo Zhang
College of Artificial Intelligence,
Nankai University
Tianjin, China

Shuhao Zhu
College of Artificial Intelligence,
Nankai University
Tianjin, China

ABSTRACT

A target tracking approach is proposed for mobile robots in this paper to address the human-robot coexistence and collaboration problem. The improved social force model (SFM) is applied to improve the tracking performance of the robot in crowded environments. When the robot approaches the pedestrians or obstacles, the tracking strategy is adaptively adjusted to avoid collision. The inverse reinforcement learning (IRL) is used to learn the parameters of the improved SFM, where the training data for the IRL is collected in real-world scenes. An effective criterion is designed to evaluate the tracking performance, which fully considers the relationship between the robot and surrounding environments. The experimental results demonstrate the effectiveness of the proposed target tracking method.

CCS CONCEPTS

• **Computer systems organization** → *Robotic autonomy*.

KEYWORDS

mobile robot, moving target tracking, social force model

ACM Reference Format:
Qinxuan Sun, Shengming Zhang, Jing Yuan*, Xuebo Zhang, and Shuhao Zhu. 2021. Moving Target Tracking with a Mobile Robot based on Modified Social Force Model. In *2021 International Conference on Robotics and Control Engineering (RobCE 2021), April 22–25, 2021, Toronto, ON, Canada.* ACM, New York, NY, USA, 5 pages. https://doi.org/10.1145/3462648.3462654

*Corresponding author.
This work was sponsored by the Natural Science Foundation of China (62073178), the Tianjin Science Fund for Distinguished Young Scholars (20JCJQJC00140, 19JCJQJC62100), the Major basic research projects of Natural Science Foundation of Shandong Province (ZR2019ZD07), the Tianjin Natural Science Foundation (20JCYBJC01470, 19JCYBJC18500), and the Fundamental Research Funds for the Central Universities, Nankai University (63206026).

Permission to make digital or hard copies of all or part of this work for personal or classroom use is granted without fee provided that copies are not made or distributed for profit or commercial advantage and that copies bear this notice and the full citation on the first page. Copyrights for components of this work owned by others than ACM must be honored. Abstracting with credit is permitted. To copy otherwise, or republish, to post on servers or to redistribute to lists, requires prior specific permission and/or a fee. Request permissions from permissions@acm.org.
RobCE 2021, April 22–25, 2021, Toronto, ON, Canada
© 2021 Association for Computing Machinery.
ACM ISBN 978-1-4503-8947-1/21/04…$15.00
https://doi.org/10.1145/3462648.3462654

1 INTRODUCTION

When the robot tracks a moving target, it will unavoidably interact with other humans as well as with the surroundings. As a result, the human-robot collaboration is an increasingly studied topic in the robotic field.

In recent years, the researches on human-robot collaboration mainly focus on the iterative re-planning-based method. In [1], the robot predicts the human motion by iteratively re-planning a trajectory based on stochastic trajectory optimizer for motion planning (STOMP). For the iterative re-planning-based method, it is vital to know how to predict the human motion. The most widely-used algorithms include the Gaussian mixture model [2–4], the hidden Markov model [5, 6], the conditional random fields [7, 8], etc. In [9], the user's gaze is monitored to predict his or her task intent based on the observed gaze patterns and the task actions are then performed according to the predictions. And in [10], the collaborative task is formulated as a two-agent planning problem and the Markov decision process (MDP) is used to model the behaviors of the robot as well as the human. In [11], the Bayesian human motion intentionality predictor (BHMIP) is proposed, which is a long-term human motion intentionality predictor based on geometric criteria. The predictor calculate the probability that a human trajectory reaches a destination to estimate the best destination.

The social force model (SFM) [12] is proposed to model the social interactions. The SFM is based on the framework of self-driven many-particle systems and simulates the pedestrian dynamics using interaction forces. The behavior of pedestrians are affected not only by the interaction forces but also by the self-driven forces. In [13], the SFM is used to investigate the mechanisms of the panic and jamming in crowds. The simulation of crowded dynamics of pedestrians are performed to prevent dangerous crowd pressure and find an optimal strategy for escape. The SFM is integrated with a multi-hypothesis target tracker in [14] to achieve more robust tracking behaviors and better occlusion handling. In [15], the SFM is used to explicitly predict the next collision in order to avoid it. In [16], the long-term behaviors of pedestrians are predicted for the robot to provide them services, which is modeled through transition probabilities between the sub-goals. And the directions to the sub-goals are decided by the collision avoiding behavior and are predicted by the SFM model. In [17], the abnormal behaviors are detected and localized in crowd videos using the SFM by placing particles over the image and estimating their interaction force. An

SFM-based control scheme is proposed in [18] for robots navigating in human scenes. The social proxemics potential field is constructed for the robots to generate and modify the path smoothly.

For the target tracking in the presence of humans or other robots, it is important to achieve harmonious coexistence between the robot and the environments. In this paper, to address the problem of interaction during the target tracking, we propose an SFM-based target tracking approach. Using the SFM, the robot can anticipatorily take actions to avoid collision when approaching pedestrians or obstacles. Thus, the coexistence and collaboration between the robot and humans can be achieved in the tracking process. The parameters of the SFM are learned through the IRL algorithm. The training data for the IRL are the pedestrian trajectories collected in various real-world scenes, which makes the SFM more adaptive to different environments in the tracking tasks. Furthermore, an effective criterion for the tracking is designed for a better evaluation of the tracking performance.

2 SOCIAL FORCE MODEL-BASED TARGET TRACKING

For the target tracking performed by mobile robots, it is unavoidable for the robots to interact with other pedestrians, the environment or the other robots. To exploit the social attribute of the robot, we apply the SFM to describe the interaction between the robot and other pedestrians as well as the obstacles to achieve a robust and efficient tracking results.

2.1 Problem Formulation

The process of target tracking is illustrated in Fig. 1(a), where P represents the current location of the moving target and R the location of the robot. The green and blue arrows indicate the moving directions of the target and robot, respectively. The angle between the moving direction of the robot and the line connecting the robot and target is denoted by φ. The kinematic model of a wheeled robot is $\dot{x}_r = v\cos\theta$, $\dot{y}_r = v\sin\theta$, and $\dot{\theta} = \omega$, where $[x_r, y_r, \theta]^T$ represents the pose of the robot w.r.t. the global coordinate system, v and ω are the linear and angular velocities of the robot, respectively. The relative location of the target w.r.t. the robot is described by the polar coordinates, as shown in Fig. 1(a). The actual distance between the robot and target is represented by r. And Q is the location where the robot is expected to arrive at and the distance between Q and P is denoted by r_d. The distance error is defined by $\tilde{r} = r - r_d$. And the corresponding dynamics can be computed by $\dot{\tilde{r}} = -v\cos\varphi$ and $\dot{\varphi} = \omega + \frac{v}{\tilde{r}+r_d}\sin\varphi$.

2.2 Social Force Model

The SFM uses interaction forces to simulate the dynamics of pedestrians. Through the application of SFM, the complicated behaviors of pedestrians can be expressed by a function based on the relative positions and velocities of the pedestrians. The SFM originally proposed in [12] is used in the simulation of crowds of interacting pedestrians. In this paper, the SFM is used to describe the interaction between the robot and pedestrians as well as obstacles. Specifically, the social force of the robot is defined by

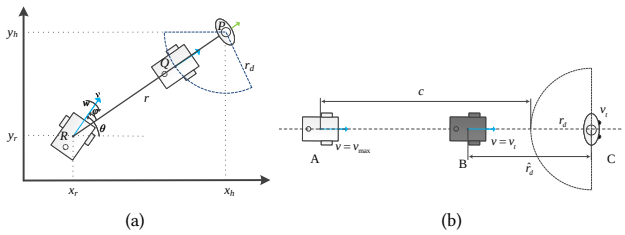

(a) (b)

Figure 1: (a) Illustration of moving target tracking by a mobile robot. (b) Illustration of adjustment of the desired tracking distance.

$F_r = f_r^0 + \sum_{i=1}^{N_p} f_{ri} + \sum_{w=1}^{N_o} f_{rw}$, where f_r^0, f_{ri} and f_{rw} represent the self-driven force for the robot, the interaction force with pedestrian i and with the obstacle w, respectively.

The self-driven force of the robot is calculated by $f_r^0 = m_r \frac{v_r^d - v_r(t)}{\tau_r}$, where m_r is the mass of the robot, v_r^d is the desired velocity, $v_r(t)$ is the actual velocity and τ_r is the time used for approaching the desired velocity. In the tracking process, the desired velocity is adjusted according to the location of the target, which is achieved by the controller defined by (1).

$$\begin{cases} v = v_{max} U(\tilde{r})\cos\varphi \\ \omega = -k\varphi - \dfrac{v_{max} U(\tilde{r})\cos\varphi}{\tilde{r} + r_d}\sin\varphi \end{cases} \tag{1}$$

The value range of k is $(0, |\omega_{max}| - \frac{v_{max}}{2r_d}]$. v_{max} and ω_{max} are the maximum linear and angular speeds of the robot, respectively, and $\tilde{r} + r_d$ is the actual distance between the robot and the target. And $U(\tilde{r})$ can be defined by

$$U(\tilde{r}) = \begin{cases} -1 & \tilde{r} < -c \\ \left(\frac{\tilde{r}+c}{c}\right)^2 - 1 & -c < \tilde{r} \le 0 \\ 1 - \left(\frac{\tilde{r}+c}{c}\right)^2 & 0 < \tilde{r} \le c \\ 1 & \tilde{r} > c \end{cases} \tag{2}$$

where c is a pre-defined constant. By use of the controller (1), when the robot is far from the target, it will move to the target at high speed to compensate for the tracking distance error. When the distance between the robot and the target reaches the desired distance r_d, the robot will slow down to ensure both the efficiency and safety.

In addition, the desired distance r_d is adjusted according to the moving speed of the target. Assume that the target is in front of the robot and they are moving in the same direction, as illustrated in Fig. 1(b). The robot begins to reduce the speed at the location A, and when it reaches the location B, the speed of the robot is equal to that of the target, i.e., $v = v_t$, with v_t representing the moving speed of the target. The desired tracking distance is calculated by $\hat{r}_d = r_d + c(1 - \sqrt{1 - \frac{v_t}{v_{max}}})$. Therefore, the desired tracking distance increases along with the moving speed v_t of the target, which avoids the possible collisions when the target is moving at a high speed and guarantee the safety in the tracking procedure.

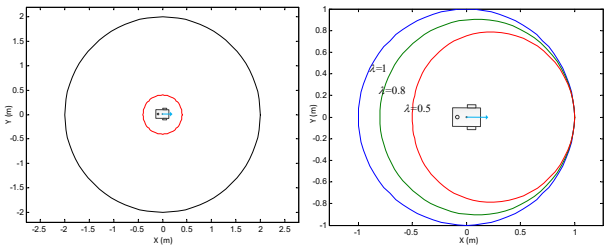

(a) (b)

Figure 2: (a) Division of the space around the robot according to the taxonomy of distances. (b) Isolines of the weight w when λ is set to different values.

The interaction force with the pedestrians is composed of three parts, i.e., the repulsive interaction force $\boldsymbol{f}_{ri}^{rep}$, the body force $\boldsymbol{f}_{ri}^{bd}$ and the sliding friction force $\boldsymbol{f}_{ri}^{fri}$, as defined by $\boldsymbol{f}_{ri} = \boldsymbol{f}_{ri}^{rep} + \boldsymbol{f}_{ri}^{bd} + \boldsymbol{f}_{ri}^{fri}$.

The repulsive interaction force $\boldsymbol{f}_{ri}^{rep}$ is calculated by

$$\boldsymbol{f}_{ri}^{rep} = (w + \mu)A_i \exp\left(\frac{r_{ri} - d_{ri}}{B_i}\right)\boldsymbol{n}_{ri}, \tag{3}$$

where A_i and B_i are constants characterizing the strength and range of the interaction force, respectively, d_{ri} denotes the distance between the robot and the pedestrian i, $\boldsymbol{n}_{ri}$ is the normalized vector pointing from the robot to the pedestrian i, and $r_{ri} = r_r + r_i$ is the sum of their radii r_r and r_i. The weights w and μ measures the degree that the interaction force is affected by the orientation and the motion tendency, respectively, which are described in detail in the following.

Based on the concept of proxemics proposed in [19], the space around a robot can be divided according to the taxonomy of distances, as shown in Fig. 2(a). In addition to the distance between the robot and the pedestrians, the interaction force is also affected by the orientation of the robot. When a pedestrian approaches the robot from the front, it will produce larger interaction force. The property is characterized by a weighting strategy and the weight is computed by $w = \lambda + (1 - \lambda)\frac{1+\cos\varphi}{2}$, where $0 \le \lambda \le 1$ is a pre-set parameter. The larger λ is, the more the force is affected by the orientation. Fig. 2(b) shows the isolines of the weight w when λ is set to 1, 0.8 and 0.5, respectively.

Furthermore, the motion tendency of the robot and the pedestrians is also considered. When the robot and the pedestrian move toward each other, it is more likely that the collision occurs. To address the affection of the motion tendency, we introduce the motion tendency factor, which is defined by $\mu = \exp((\boldsymbol{v}_r - \boldsymbol{v}_i) \cdot \boldsymbol{n}_{ri})$, where $\boldsymbol{v}_r$ and $\boldsymbol{v}_i$ are the velocities of the robot and pedestrian i, respectively, $\boldsymbol{n}_{ri}$ is the unit vector pointing from the robot to the pedestrian. As defined in (3), when the robot and the pedestrian tend to move toward each other, the interaction force between them increases which are indicated by the value of μ.

The body force $\boldsymbol{f}_{ri}^{bd}$ is computed by $\boldsymbol{f}_{ri}^{bd} = k_1 G(r_{ri} - d_{ri})\boldsymbol{n}_{ri}$, where k_1 is a constant coefficient and $G(x) = x$ when $x > 0$, otherwise, $G(x) = 0$. And the sliding friction force $\boldsymbol{f}_{ri}^{fri}$ is calculated by

(a) (b)

Figure 3: The scenes to collect the dataset for the parameter learning of interaction with the (a) pedestrians and (b) obstacles, respectively.

$\boldsymbol{f}_{ri}^{fri} = k_2 G(r_{ri} - d_{ri})\Delta v_{ri}^t \boldsymbol{t}_{ri}$, where $\boldsymbol{t}_{ri}$ is the tangential direction and $\Delta v_{ri}^t = (\boldsymbol{v}_i - \boldsymbol{v}_r) \cdot \boldsymbol{t}_{ri}$ the tangential velocity difference.

The interaction force with the obstacle can be treated analogously and is computed by

$$\boldsymbol{f}_{rw} = \boldsymbol{f}_{rw}^{rep} + \boldsymbol{f}_{rw}^{bd} + \boldsymbol{f}_{rw}^{fri}, \tag{4}$$

$$\begin{aligned} \boldsymbol{f}_{rw}^{rep} &= (w + \mu)A_w \exp\left(\frac{r_r - d_{rw}}{B_w}\right)\boldsymbol{n}_{rw}, \\ \boldsymbol{f}_{rw}^{bd} &= k_1 G(r_r - d_{rw})\boldsymbol{n}_{rw}, \\ \boldsymbol{f}_{rw}^{fri} &= k_2 G(r_r - d_{rw})(\boldsymbol{v}_r \cdot \boldsymbol{t}_{rw})\boldsymbol{t}_{rw}. \end{aligned} \tag{5}$$

In (5), A_w and B_w represent respectively the strength and range of the interaction force, d_{rw} means the distance between the robot and the obstacle, $\boldsymbol{n}_{rw}$ denotes the normalized vector pointing from the robot to the obstacle, and $\boldsymbol{t}_{rw}$ is the direction tangential to $\boldsymbol{n}_{rw}$.

3 IRL-BASED PARAMETER LEARNING FOR SFM

In this paper, we use the IRL to learn the parameters of the SFM. The training data for the IRL is collected at the College of Artificial Intelligent in Nankai University and the camera used for data capture is Sony IMX362 with a focal length of 3.94mm. The collection scene for the parameter learning of interaction with the pedestrians is shown in Fig. 3(a) and the camera is positioned at a height of 5.16m.. Two entrances into the hall are labeled by "1" and "2", respectively, the stairs leading to the 2nd floor is labeled by "3", and the corridor leading to other rooms in this floor is labeled by "4". Most of the pedestrians walks from location 1 or 2 to location 3 or 4, or vice versa, as shown in Fig. 3(a). The scene for the parameter learning of interaction with the obstacles is shown in Fig. 3(b) and the camera is positioned at a height of 1.6m. Pedestrians enter the scene through the entrance labeled "5" and leave it through "6", or vice versa.

The pixel coordinates of a pedestrian is computed for each image from the dataset, which are denoted by $\boldsymbol{u}_k$ in the k-th frame. The corresponding 3D coordinates $\boldsymbol{x}_k$ of the pedestrian in the camera coordinate system can be computed by the method proposed in [20]. The trajectory of the pedestrian can then be denoted by $X = \{\boldsymbol{x}_1, \boldsymbol{x}_2, \cdots, \boldsymbol{x}_N\}$, where N is the number of images in which the pedestrian appears. And the instant velocity of the pedestrian can be calculated by $\boldsymbol{v}_k = \frac{\boldsymbol{x}_{k+1} - \boldsymbol{x}_k}{\Delta t_k}$, where Δt_k is the time interval between the k-th and $k+1$-th frames.

Table 1: Results of the SFM parameter learning.

Parameter	A_i	B_i	A_w	B_w
Mean	8.50	0.56	5.50	0.44
Std.	5.10	0.20	2.10	0.21

Figure 4: The simulated trajectory (blue) based on the SFM parameters learned by IRL compared against the real trajectory (red) of the pedestrian.

For the trajectory X, the position $\boldsymbol{x}_k^s$ of the pedestrian at each step can be simulated using the improved SFM introduced in Section 2.2. The reward function of IRL for the SFM parameter learning are defined by $\{A_i, B_i, A_w, B_w\} = \arg\min_{\{A_i, B_i, A_w, B_w\}} \sum_k \|\boldsymbol{x}_k^s - \boldsymbol{x}_k\|$. The results of the SFM parameter learning are listed in Fig. 1. Fig. 4 shows the simulated trajectory based on the SFM with the learned parameters compared against the real trajectory of the pedestrians. It can be seen that the two trajectories almost overlap with each other, which demonstrates the effectiveness of the IRL-based SFM parameter learning.

4 SIMULATION AND EVALUATION

In this section, an effective criterion is designed for the evaluation of the target tracking performance. Then, the simulations are performed on the improved SFM-based robot motion generation and target tracking.

4.1 Evaluation Criterion

For a more effective evaluation of the target tracking, the criterion is designed considering not only the distance and relative orientation between the robot and target, but also the relationships between the robot and other pedestrians or obstacles in the tracking process.

As illustrated in Fig. 1(a), the distance and relative orientation between the robot and target are important criteria for the evaluation of tracking performance. If the robot comes too close to the target, it is possible to collide with each other, which yields a threat to safety. If the robot is far from the target, or if the target is out of the FoV of the robot, it is likely for the robot to lose track of the target. As a result, it is necessary to keep the suitable tracking distance and orientation. Furthermore, the relative moving speed of the robot w.r.t. the target is also significant in the tracking process. Assume that the speeds of the robot and target are v_r and v_p, respectively, and the relative speed is computed by $\Delta v = |v_r - v_p|$. The utility function of the relative speed is defined by $f_v = \exp(-\Delta v)$. The value of the utility function increases along with the decrease of the relative speed, indicating that the robot keeps tracking the target in a stable state.

In addition to the tracking target, the relative relationships with the surrounding environments are also important in the tracking tasks of mobile robots. The minimum distance between the robot and the closest obstacle or pedestrian is denoted by d_{min}. The corresponding utility function is defined by $f_h = \frac{d_{min}}{2}$ when $d_{min} \leq 2$, and otherwise $f_h = 1$. The value of the function indicate the influences of the surrounding environments to the tracking tasks of the robot.

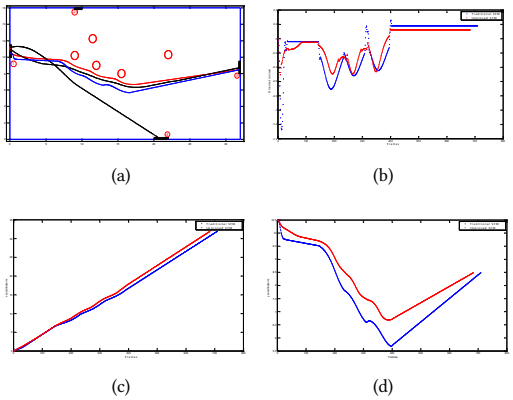

Figure 5: (a) Trajectories of the robot simulated using the improved SFM (red) and traditional SFM (blue), as well as the trajectories of pedestrians (black). (b) Orientation, (c) x and (d) coordinates of the robot simulated using the improved SFM (red) and traditional SFM (blue).

4.2 Robot Motion Simulation based on Improved SFM

In this subsection, we use the improved SFM to generate the motion of a mobile robot in a simulated hall environment in Fig. 5(a). The hall has four entrances, which is labeled by "1", "2", "3" and "4", respectively, and the obstacles are represented by red circles with a radius of 0.5m. In the experiment, two pedestrians are randomly generated in the tracking process and the robot is supposed to reach the goal without colliding with the pedestrians/obstacles or disturbing the motion of the pedestrians. Fig. 5(a) shows the trajectories of the robot using the improved and traditional SFM, as well as the trajectories of the pedestrians. The orientation and position of the robot is plotted in Fig. 5(b)(c)(d), respectively. It can be seen that the improved SFM with parameters learned by the IRL algorithm generates more smooth and anticipatory motion for the robot.

4.3 Target Tracking based on Improved SFM

The improved SFM with parameters learned by the IRL algorithm is applied to the target tracking task of the mobile robot and is compared with the tracking based on the controller defined by (1). The experiments are executed in the simulated environment in Fig. 5(a) and three pedestrians are randomly generated in the

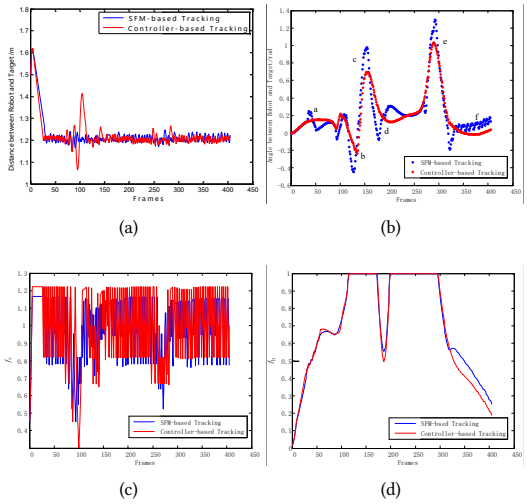

Figure 6: Comparison results of target tracking.

simulation. The relative distance and angle between the robot and target are plotted in Fig. 6(a) and (b), respectively. For the SFM-based target tracking, when the robot approach the pedestrians or obstacles, the orientation is adjusted to avoid any possible collision. And the values of utility functions defined in Section 4.1 are plotted in Fig. 6 (c) and (d), respectively. In the SFM-based tracking, the velocity of the robot is more similar with that of the target, which increases the safety and comfort of the complete human-robot system. In summary, compared with the controller-based tracking, the improved SFM is more suitable for the target tracking task for mobile robots.

5 CONCLUSION

In this paper, a target tracking approach based on the improved SFM is proposed to achieve the harmonious coexistence and collaboration between the robot and pedestrians. Compared with the traditional SFM, the parameters of the improved SFM are learned through the IRL algorithm, which significantly improve the adaptability and flexibility of the SFM-based tracking. An effective criterion is designed to evaluate the target tracking performance. The experimental results show the efficiency and robustness of the proposed method.

REFERENCES

[1] J. Mainprice, R. Hayne, and D. Berenson. 2016. Goal Set Inverse Optimal Control and Iterative Replanning for Predicting Human Reaching Motions in Shared Workspaces. *IEEE Transactions on Robotics* 32, 4 (2016), 897–908. https://doi.org/10.1109/TRO.2016.2581216

[2] M. Ewerton, G. Neumann, R. Lioutikov, H. Ben Amor, J. Peters, and G. Maeda. 2015. Learning multiple collaborative tasks with a mixture of Interaction Primitives. In *2015 IEEE International Conference on Robotics and Automation (ICRA)*. 1535–1542. https://doi.org/10.1109/ICRA.2015.7139393

[3] A. D. Wilson and A. F. Bobick. 1999. Parametric hidden Markov models for gesture recognition. *IEEE Transactions on Pattern Analysis and Machine Intelligence* 21, 9 (1999), 884–900. https://doi.org/10.1109/34.790429

[4] J. Mainprice and D. Berenson. 2013. Human-robot collaborative manipulation planning using early prediction of human motion. In *2013 IEEE/RSJ International Conference on Intelligent Robots and Systems*. 299–306. https://doi.org/10.1109/IROS.2013.6696368

[5] L. Bretzner, I. Laptev, and T. Lindeberg. 2002. Hand gesture recognition using multi-scale colour features, hierarchical models and particle filtering. In *Proceedings of Fifth IEEE International Conference on Automatic Face Gesture Recognition*. 423–428. https://doi.org/10.1109/AFGR.2002.1004190

[6] Dana Kulić, Christian Ott, Dongheui Lee, Junichi Ishikawa, and Yoshihiko Nakamura. 2012. Incremental learning of full body motion primitives and their sequencing through human motion observation. *The International Journal of Robotics Research* 31, 3 (2012), 330–345. https://doi.org/10.1177/0278364911426178

[7] H. S. Koppula and A. Saxena. 2016. Anticipating Human Activities Using Object Affordances for Reactive Robotic Response. *IEEE Transactions on Pattern Analysis and Machine Intelligence* 38, 1 (2016), 14–29. https://doi.org/10.1109/TPAMI.2015.2430335

[8] Yun Jiang and Ashutosh Saxena. 2014. Modeling High-Dimensional Humans for Activity Anticipation using Gaussian Process Latent CRFs, In Robotics: Science and Systems. *IEEE Transactions on Pattern Analysis and Machine Intelligence*.

[9] C. Huang and B. Mutlu. 2016. Anticipatory robot control for efficient human-robot collaboration. In *2016 11th ACM/IEEE International Conference on Human-Robot Interaction (HRI)*. 83–90. https://doi.org/10.1109/HRI.2016.7451737

[10] Hema S. Koppula, Ashesh Jain, and Ashutosh Saxena. 2016. *Anticipatory Planning for Human-Robot Teams*. Springer International Publishing, Cham, 453–470. https://doi.org/10.1007/978-3-319-23778-7_30

[11] Gonzalo Ferrer and Alberto Sanfeliu. 2014. Bayesian Human Motion Intentionality Prediction in urban environments. *Pattern Recognition Letters* 44 (2014), 134 – 140. https://doi.org/10.1016/j.patrec.2013.08.013 Pattern Recognition and Crowd Analysis.

[12] Dirk Helbing and Peter Molnar. 1998. Social Force Model for Pedestrian Dynamics. *Physical Review E* 51 (05 1998). https://doi.org/10.1103/PhysRevE.51.4282

[13] Dirk Helbing, Illés Farkas, and Tamás Vicsek. 2000. Simulating dynamical features of escape panic. *Nature* 407, 6803 (01 Sep 2000), 487–490. https://doi.org/10.1038/35035023

[14] M. Luber, J. A. Stork, G. D. Tipaldi, and K. O. Arras. 2010. People tracking with human motion predictions from social forces. In *2010 IEEE International Conference on Robotics and Automation*. 464–469. https://doi.org/10.1109/ROBOT.2010.5509779

[15] F. Zanlungo, T. Ikeda, and T. Kanda. 2011. Social force model with explicit collision prediction. *EPL (Europhysics Letters)* 93, 6 (mar 2011), 68005. https://doi.org/10.1209/0295-5075/93/68005

[16] Tetsushi Ikeda, Yoshihiro Chigodo, Daniel Rea, Francesco Zanlungo, Masahiro Shiomi, and Takayuki Kanda. 2012. Modeling and Prediction of Pedestrian Behavior based on the Sub-goal Concept. In *Proceedings of Robotics: Science and Systems*. Sydney, Australia. https://doi.org/10.15607/RSS.2012.VIII.018

[17] R. Mehran, A. Oyama, and M. Shah. 2009. Abnormal crowd behavior detection using social force model. In *2009 IEEE Conference on Computer Vision and Pattern Recognition*. 935–942. https://doi.org/10.1109/CVPR.2009.5206641

[18] C. Wang, Y. Li, S. S. Ge, and T. H. Lee. 2016. Adaptive control for robot navigation in human environments based on social force model. In *2016 IEEE International Conference on Robotics and Automation (ICRA)*. 5690–5695. https://doi.org/10.1109/ICRA.2016.7487791

[19] Edward Twitchell Hall. 1990. *The hidden dimension*. Anchor Books.

[20] J. Yuan, H. Chen, F. Sun, and Y. Huang. 2015. Multisensor Information Fusion for People Tracking With a Mobile Robot: A Particle Filtering Approach. *IEEE Transactions on Instrumentation and Measurement* 64, 9 (2015), 2427–2442. https://doi.org/10.1109/TIM.2015.2407512